Adaptation to AI therapy in breast cancer can induce dynamic alterations in ER activity resulting in estrogen independent metastatic tumours

Adaptation to AI therapy in breast cancer can induce dynamic alterations in ER activity resulting in estrogen independent metastatic tumours

Damir Varešlija[1*], Jean McBryan[1*], Ailís Fagan[1], Aisling M. Redmond[2], Yuan Hao[3], Andrew H. Sims[4], Arran Turnbull[5], J.M. Dixon[5], Peadar Ó'Gaora[6], Lance Hudson[1], Siobhan Purcell[1], Arnold D.K. Hill[1] and Leonie S. Young[1].

*These authors contributed equally to this work.

[1]Endocrine Oncology Research Group, Department of Surgery, Royal College of Surgeons in Ireland, Dublin 2, Ireland.

[2]Cancer Research UK Cambridge Institute, University of Cambridge, Li Ka Shing Centre, Robinson Way, Cambridge CB2 0RE, UK.

[3]Cold Spring Harbor Laboratory, 1 Bungtown Rd, Cold Spring Harbor, New York. 11724.

[4]University of Edinburgh Cancer Research UK Building, Carrington Crescent, Edinburgh EH4 2XR, UK.

[5]Breakthrough Breast Research Laboratories, Edinburgh, EH4 2XU, UK.

[6]Biomolecular and Biomedical Science, Conway Institute, University College Dublin, Dublin, Ireland.**Corresponding author:** Leonie Young, Department of Surgery, Royal College of Surgeons in Ireland, Dublin 2, Ireland. Tel: +353 1 4028576. lyoung@rcsi.ie

Running title: Dynamic ER adaptation to AI therapy

Key words: ER Chip-seq; AI resistance; neo-adjuvant; Relapse; Matched Metastatic Tumours

Conflict of interest: The authors declare there is no conflict of interest.

Word Count: 5,399

Total number of figures and/or tables: 6

STATEMENT OF TRANSLATIONAL RELEVANCE

Aromatase inhibitors (AIs) are the treatment of choice for postmenopausal women with ER positive breast tumours. Although effective, resistance to AIs, through various mechanisms, is an ongoing clinical problem.

The current study is the first to profile ER activity in the estrogen depleted AI resistant setting. Rather than being silenced in response to AI therapy, the ER can undergo dynamic adaptations to regulate transcription in an estrogen-independent manner. Furthermore, by the time metastatic disease has developed, a small but significant subset of tumours has adapted to survive without ER activity.

From the clinical perspective, this study highlights two important issues: firstly, the need for more efficient drugs to completely block ER signalling; and secondly, the need to re-assess where possible, the ER status during disease progression, particularly at the metastatic stage, in order to select the most appropriate treatment.

ABSTRACT

Purpose: Acquired resistance to aromatase inhibitor therapy is a major clinical problem in the treatment of breast cancer. The detailed mechanisms of how tumour cells develop this resistance remain unclear. Here, the adapted function of ER to an estrogen-depleted environment following AI treatment is reported.

Experimental Design: Global ER-ChIPseq analysis of AI resistant cells identified steroid-independent ER target genes. Matched patient tumour samples, collected before and after AI treatment, were used to assess ER activity.

Results: Maintained ER activity was observed in patient tumours following neoadjuvant AI therapy. Genome-wide ER-DNA binding analysis in AI resistant cell lines identified a subset of classic ligand dependent ER target genes which develop steroid independence. Kaplan Meier analysis revealed a significant association between tumours which fail to decrease this steroid independent ER target gene set in response to neoadjuvant AI therapy, and poor disease-free and overall survival (n=72 matched patient tumour samples, p=0.00339 and 0.00155 respectively). The adaptive ER response to AI treatment was highlighted by the ER/AIB1 target gene, early growth response 3 (EGR3). Elevated levels of EGR3 were detected in endocrine resistant local disease recurrent patient tumours in comparison to matched primary tissue. However, evidence from distant metastatic tumours demonstrates that the ER signalling network may undergo further adaptations with disease progression as estrogen-independent ER target gene expression is routinely lost in established metastatic tumours.

Conclusions: Overall, these data provide evidence of a dynamic ER response to endocrine treatment which may provide vital clues for overcoming the clinical issue of therapy resistance.

INTRODUCTION

Aromatase inhibitor (AI) therapy is now the first line treatment for ER positive post-menopausal breast cancer patients. With prolonged exposure, a significant number of patients develop AI resistance (1). Several molecular mechanisms of acquired resistance have been described and these include enhanced signalling through growth factor pathways as well as ligand-independent estrogen receptor (ER) function (2, 3).

ER/growth factor cross talk and in particular amplification of the growth factor receptor HER2 has been associated with resistance to endocrine therapy in both preclinical and clinical studies (4-6). Recently, clinical and proteomic work has implicated Phosphoinositide (PI) 3-kinase as a central node in AI resistant second messenger signalling networks (2, 7-9). Activation of PI3-kinase has been shown to induce ER phosphorylation and promote estrogen independent ER transcriptional activity (10, 11). However, molecular studies in models of AI resistance suggest that PI3-kinase may not be directly responsible for ligand-independent ER signalling following prolonged steroid deprivation (12).

Clinical trial data which describes the efficacy of the ER disrupter fulvestrant as a second-line therapy in patients who progressed on an AI treatment suggests that a functional ER remains after development of AI resistance (13, 14). Though molecular studies have suggested that mutations in the ligand binding domain may be important in determining response to endocrine therapy (15, 16), ER mutations in primary patient breast cancers were found to be uncommon (17). More recently however, reports are emerging of ligand binding domain ER mutations in endocrine related metastasis which can confer estrogen independent activity of the receptor and contribute to the development of resistance (18, 19). Furthermore, global analysis of ER binding events has revealed altered DNA binding dynamics and a gain of new target genes in tumours from patients with a poor response to treatment (20).

Clinical and sequencing data describing somatic mutations and altered ER activity do not fully explain continued metastatic disease progression. There is now evidence that a functioning ER may not be required for sustained tumour growth at

established metastatic sites in all patients. Receptor switching between the primary and secondary tumours in ER positive breast cancer has been reported, with up to 20% of tumours losing ER and/or PR with a reciprocal gain of HER2 (21-23). These clinical data raise the possibility that once metastatic tumours have formed, a significant number of these become steroid receptor independent.

In this study we investigate the functional and clinical consequences of altered ER action in response to prolonged estrogen deprivation. In a model of resistance to the AI letrozole, we report a global loss of ER binding and identify a subset of classic ligand dependent ER target genes which become estrogen independent. Initial adaptation to estrogen deprivation, manifested by ligand independent ER activation, is found to contribute to the development of local endocrine resistance *in vitro*. At a clinical level failure to regulate the steroid independent ER gene set following neoadjuvant treatment associates with poor long-term response to AI therapy in breast cancer patients. Further ER adaptation can occur with the establishment of metastatic tumours, where loss of ER function and target gene expression can lead to the development of a fully estrogen independent endocrine resistant tumour.

MATERIALS AND METHODS

Cell lines and treatments

Endocrine-sensitive MCF7 breast cancer cells were obtained from American Type Culture Collection (ATCC). Endocrine-resistant LY2 cells were a kind gift from R. Clarke, Georgetown University, Washington DC (24). Cells were grown as previously described (25). Aromatase inhibitor sensitive cells (MCF7-Aro) were developed by stable transfection of the aromatase gene (CYP19) (Invitrogen). MCF7-Aro cells were cultured in MEM supplemented with 10% FCS, 1% L-Glutamine, 1% Pen/Strep, and 200 mg/mL Geneticin (G418, Gibco Invitrogen). AI-resistant (LetR and AnaR) cells were generated by long-term culture of MCF7-Aro cells with an AI (letrozole, 10^{-6}M, Novartis or anastrozole, 10^{-6}M, AstraZeneca) and androstenedione (25 x 10^{-9} M, Sigma Aldrich) in MEM supplemented with 10% charcoal-dextran-stripped FCS, 1% L-Glutamine, 1%

Pen/Strep, and 200 mg/mL Geneticin. Cells were maintained in steroid depleted medium (phenol red-free MEM with 10% charcoal-dextran stripped FCS, 1% Glutamine and 1% Pen/Strep) for 72 hours prior to treatment with hormones (estradiol, 10^{-7}M, Sigma Aldrich or androstenedione, 10^{-7} M, Sigma Aldrich), or letrozole (10^{-6} M, Novartis). All cells were maintained at 37^{0}C, 5% CO_2 in a humidified incubator. All cell lines were authenticated according to ATCC guidelines (Supplementary Table S1).

Transfections

SiRNA directed against AIB1 (Ambion, AM16706 and Dharmacon L-003759-00-0005), ERα (Ambion, 4392421 and Dharmacon, LQ-003401-00-0002) and EGR3 (Qiagen, GS1960) were used to knock down gene expression. Multiple siRNAs from the EGR3 and ER SMARTpools were compared and the most effective was selected for further studies (EGR3 siRNA-6 and ER siRNA-4) (Supplementary Fig. S1 and S2). Transfections were carried out using Lipofectamine 2000 (Invitrogen) as per manufacturer's instructions.

Cell growth and cell motility assays

Cellomics Cell Motility Kit (Thermo Scientific, K0800011) was used to assess individual cell movement after 24 hours as per manufacturer's instructions using cells seeded at $1x10^{4}$cells/mL. Mean track areas (minimum of 90 cell tracks per condition) were analyzed with Olympus cell imaging software and compared with a Student t test.
For growth assays, following steroid depletion, cells were transfected with siRNA of interest, and then 24 hours later seeded out into 12-well plates at $2x10^{4}$cells/mL. The cells were counted manually using a haemocytometer at three different time points. Cell numbers were compared by Student t test.

Chromatin immunoprecipitation (ChIP)

ChIP experiments were performed as described previously (26). Antibodies used were anti-ER (sc-543) from Santa Cruz Biotechnologies and AIB1 (sc-25742). LetR cells were treated with vehicle or androstenedione and MCF7 cells were treated with vehicle

or estrogen for 45 minutes, cross-linked with 1% formaldehyde (F15587, Sigma Aldrich) for ten minutes and scraped into PBS with protease inhibitors (Complete Mini, Roche). Immunoprecipitation was performed using an antibody attached to Dynal beads (Dynabeads® M-280 Sheep Anti-Rabbit IgG, Life Technologies). The proteins were then removed from the DNA by reverse crosslinking overnight and the DNA was extracted using phenol-chloroform-isoamyl alcohol (P2069, Sigma Aldrich). Real-time PCR was carried out in duplicate by SYBR Green PCR (Qiagen) using a Lightcycler (Roche) and primers are listed in Supplementary Table S2.

ChIP-seq

Cells were treated and harvested for ChIP-seq as described previously (26). Immunoprecipitation was carried out using an anti-ER antibody (sc-543) attached to Dynal beads (Dynabeads® Protein A 10001D, Life Technologies). ChIP DNA was amplified as described (26), and sequenced using the Illumina Genome Analyzer-II system. Single end 36-bp ChIP-seq data were generated by the Illumina analysis pipeline version 1.6.1. ChIP-seq data from this study has been deposited in the NCBI Gene Expression Omnibus (GEO) (http://www.ncbi.nlm.nih.gov/geo/) under accession number GSE54592. LY2 and MCF7 ER ChIPseq data has previously been reported and can be found in ArrayExpress (www.ebi.ac.uk/arrayexpress/) under accessions E-MTAB-1865 and E-MTAB-223 respectively (27, 28).

Bioinformatics

ChIP-seq reads were aligned to the hg19 genome using Bowtie (v0.12.9) (29). Bowtie parameters were set to allow reads to be aligned to the genome if they mapped to one region only and if they had less than 2 base pair mismatches. MACS (v2.0) was applied to the ChIP-seq alignments to call peak regions (30). Peaks were called using a p-value cut-off of 1e-03. Bioinformatic analyses are described in the Supplementary Methods.

Expression studies

RNA isolation and cDNA synthesis were performed as previously described (31). Real-time PCR was carried out either by SYBR Green PCR (Qiagen) using a Lightcycler (Roche) or by TaqMan probe technology (Applied Biosystems), on the ABI PRISM 7500 platform. The comparative C_T ($\Delta\Delta C_T$) method was applied to analyse relative gene expression levels. Primer and probe details are outlined in Supplementary Table S2.

Protein blotting

Protein from breast cancer cells was lysed, electrophoresed and immunoblotted with the following antibodies: ER (mouse, NCL-L-ER-6F11, Leica Biosystems), AIB1 (rabbit, sc-25742; Santa Cruz), EGR3 (rabbit, sc-191, Santa Cruz), MREG (mouse, sc-374216, Santa Cruz), FOXA1 (ab23738, Abcam), β-ACTIN (ab6276, Abcam).

Patient information and construction of tissue microarray

Patient breast tumour samples for the tissue microarray (TMA) were collected and data recorded as previously described (32). Data included: pathologic characteristics (tumour stage, grade, lymph node status, ER status, recurrence) and treatment with radiotherapy, chemotherapy, tamoxifen, or AIs. Detailed follow-up data (median, 51 months) were collected on the patients to monitor recurrences. TMAs were constructed as described previously (25).

Immunohistochemistry

Immunohistochemistry (IHC) was carried out using antibodies against EGR3 (1:500, rabbit, sc-191, Santa Cruz), pSer118 ER (1:500, mouse, mAB2511, Cell Signalling), AIB1 (3:200, rabbit, sc-25742, Santa Cruz), ki67 (1:200,mouse, M7240, DAKO), AR (1:50, mouse, 318-CE, Novacastra) and ER (1:50, rabbit, 790-4324, Ventana Medical Systems) with the Dako EnVision™ Kit (31). Antigen retrieval was done with either EDTA or

sodium citrate. Primary antibody was used at the recommended dilution and incubated for 1 hour at room temperature or overnight at 4°C in the case of pSer118. Staining was assessed using a modified Allred scoring system as previously described (33). Independent observers, without knowledge of prognostic factors, scored slides. Staining was also assessed by the Aperio IHC Nuclear Image Analysis algorithm (Leica Biosystems). Paired t-tests were used to compare differences in expression between matched tumour samples.

Statistical analysis

Associations of EGR3 with clinicopathologic variables were examined using Fisher exact test. Statistical analyses were conducted using STATA 10 data analysis software (Stata Corp. LP) and GraphPad Prism 6 (GraphPad software Inc,) and values of $p<0.05$ were considered significant. Changes in gene expression on AI treatment and association with outcome were determined from the Edinburgh dataset of 72 patients treated with letrozole, performed on Affymetrix and Illumina microarrays with batch correction (34, 35). Kaplan Meier analysis was performed using the R Survival package. The Cluster and TreeView programs were used to generate heat maps.

RESULTS

Aromatase inhibitor therapy can induce ligand independent ER activity. Steroid receptor expression was maintained in breast cancer tissue from patients following neoadjuvant treatment in comparison to matched pre-treatment biopsies (Supplementary Table S3; Supplementary Fig. S3 and S4). However, enhanced pSer118 ER was detected in post-treatment tissue indicating induction of ligand independent ER activity, (n=8 breast cancer patients, p=0.002) (Fig. 1A, Supplementary Table S3 and Supplementary Fig. S3). Consistent with this observation, in cell models of resistance to the AI therapies (letrozole resistant LetR cells and anastrozole resistant AnaR cells), ER was found to be required for cell growth even in the absence of steroids. By contrast, knockdown of ER in a steroid-free environment in endocrine sensitive cells (MCF7 and

MCF7-Aro), had no impact on tumour cell number (Fig. 1B, Supplementary Fig. S1 and S2). The AI resistant cell lines express higher levels of pSer118 ER than the sensitive cells (31).Taken together, these data indicate that reduced estrogen as a result of AI treatment can lead to enhanced ligand independent ER activity.

The estrogen receptor develops steroid-independent functional activity in AI resistant cells. To examine the consequence of ER signalling following AI treatment we investigated global ER signalling in the AI resistant setting. ER ChIP-seq was performed in AI resistant breast cancer cells (LetR) in the presence and absence of androstenedione. Analysis of genome wide ER-DNA binding events revealed that, similar to tamoxifen resistance, ER binding events were observed to be less frequent in AI resistant cells in comparison to those published for endocrine sensitive MCF7 cells (27). Furthermore, steroid treatment did not result in any enhancement in ER-DNA interactions in the LetR cells (Fig. 2A), supporting a role for ligand independent ER activation in AI resistant cells. Examination of the ER binding regions identified from LetR cells in other endocrine models (MCF-7 and LY2 cells), confirms reduced ligand dependency as a feature of ER activity in endocrine resistance (Supplementary Fig. S5).

ER binding peaks in LetR cells were significantly enriched for ERE, FOXA1 and GATA3 binding motifs (Supplementary Table S4). In addition, interactions between ER and FOXA1 were found to be unaltered in LetR cells compared to MCF7 cells indicative of a fully functional core ER-DNA complex (Supplementary Fig. S6). Previous studies from our group have observed that steroid-independent ER activity in AI resistance can occur in a promoter-specific context (31). To investigate this at a global level, the prevalence of transcription factor (TF) binding motifs within the ER binding peaks were compared between peaks that are unique to the vehicle treated sample, unique to the androgen-treated sample or common to both (Fig. 2B and C). Estrogen response elements (EREs) were found to be significantly enriched in the steroid-independent setting (vehicle only and common peaks) compared to the steroid-driven setting (androstenedione only

peaks). In contrast, the steroid-driven peaks were enriched for Forkhead motifs such as FOXA1 (Fig. 2C, Supplementary Table S5).

Steroid independent target genes identified from ER ChIP-seq data from this study were compared with steroid sensitive ER target genes from public microarray data sets (estrogen treated MCF7 cells and testosterone treated MCF7-Aro cells) (32, 33). The gene set was refined based on common expression in a second independent LetR gene set (36). This analysis defined a set of ER target genes which have become steroid dysregulated in AI resistance (Fig. 2D). The set of steroid dysregulated genes are GREB1, TFF1, EGR3, MREG, TPD52L1, SIAH2 and MYB, which from hereon are referred to as the ER target gene signature (Fig. 2D and Supplementary Fig. S7). Of interest, ChIP-seq in LY2 cells confirmed that these genes are also steroid independent ER targets in the tamoxifen resistant setting (Supplementary Fig. S8).

The estrogen receptor regulates target genes EGR3 and MREG independently of steroids in AI resistant cells. The ability of AI resistant cells to regulate ER signalling in a ligand-independent manner was investigated with in depth studies on selected targets, EGR3 and MREG. EGR3 is a transcription factor and an early growth response gene while MREG or melanoregulin is a membrane protein named for its involvement in melanocyte differentiation. Both of these genes contain an ERE within the ER binding peak (Fig. 3A). ChIP confirmed estrogen-dependent ER recruitment in MCF7 cells and strong recruitment, independent of androgen treatment, in LetR cells, to the DNA of these gene targets (Fig. 3B). Furthermore, ER knockdown using siRNA resulted in reduced mRNA and protein expression of both EGR3 and MREG (Fig. 3C). Of interest, the binding peak located proximal to the transcriptional start site of EGR3 is located within another gene, PEBP4. Knockdown studies confirmed that ER binding regulates transcriptional activity of EGR3 but not PEBP4 (Supplementary Fig. S9). Treatment of MCF7 cells with estrogen resulted in marked upregulation of EGR3 and MREG at both mRNA and protein levels (Fig. 3D). By contrast, vehicle-treated LetR cells had high basal

expression of EGR3 and MREG and treatment with androgen did not induce significant further regulation (Fig. 3D).

AIB1 binds to the DNA at the same location as ER to regulate expression of both EGR3 and MREG. The steroid receptor co-activator, AIB1, is well known to cooperate with ER in regulating expression of target genes. The globally identified ER target genes in LetR cells were analysed for the presence of AIB1 binding sites using publicly available data from AIB1 ChIP-seq in MCF7 cells (37). 75% of identified ER binding regions in LetR cells overlapped with AIB1 binding peaks. The ER binding peaks which had become independent of steroids were enriched for AIB1 binding sites compared to those peaks which remained steroid regulated (Fig. 4A), suggesting a potential role for AIB1 in ligand independent ER activity. For EGR3 and MREG, ChIP confirmed recruitment of AIB1 to the ER-DNA loci (Fig. 4B). As predicted, this recruitment was regulated by estrogen in MCF7 cells, but was steroid independent in LetR cells (Fig. 4B). Silencing of AIB1 resulted in reduced transcript and protein expression of both EGR3 and MREG, confirming the transcriptional function of AIB1 binding to the DNA (Fig. 4C, Supplementary Fig. S2). Thus AIB1 appears to retain its steroid receptor coactivator role in AI resistant cells and functions to co-regulate expression of ER target genes in the absence of steroid.

Previous studies reported a significant association between AIB1 expression in breast cancer tissue and reduced disease free survival in AI treated patients (31). In this study we observed a strong correlation between AIB1, ER and EGR3 (EGR3-ER, n=375, $p<0.0001$; EGR3-AIB1, n=212, $p<0.0001$; AIB1-ER, n=212, $p<0.0001$) in the primary tumours of breast cancer patients (Fig. 4D, Supplementary Table S6).

Patient treatment with AIs induces an early response in expression of ER target gene signature. The current use of AIs as a neoadjuvant therapy allows real-time sampling and monitoring of tumour responses to endocrine therapy (Fig. 5A). Expression of our ER target gene signature was examined in a cohort of matched

tumour biopsies from 50 letrozole treated patients before, two weeks during and three months following neo-adjuvant AI treatment (published dataset GSE20181) (Fig. 5B) (38). Treatment with AI therapy reduced expression of the dysregulated gene set, with the exception of EGR3 (Fig. 5B). For the genes TFF1, GREB1, MREG, SIAH2 and MYB, the decrease in expression was statistically significant (n=50, p-value <0.0001).

For the gene EGR3 after an initial loss at 2 weeks treatment (n=50, p=0.0016), a significant increase in EGR3 transcript was seen following 3 months neoadjuvant therapy (p=0.0001) (Fig. 5B). This observation was confirmed at the protein level by immunohistochemistry of tumour tissue from an independent cohort of AI treated patients (n=9, p=0.0002) (Fig 5C, Supplementary Table S3). The response to AI therapy was modelled *in vitro* where enhanced EGR3 expression observed following acute 4 hours androstenedione treatment was inhibited by letrozole, whereas sustained 3 month co-treatment with the steroid and the AI inhibitor failed to reduce EGR3 expression (Fig. 5D).

At a functional level *in vitro* studies in models of AI resistance confirm a role for EGR3 in proliferation and migration of endocrine resistant cells (Supplementary Fig. S10). In the patient setting, the clinical significance of the gene response to neoadjuvant AI therapy was examined in an extended cohort of 72 paired tumour biopsies with 10 year follow up data (published datasets GSE20181, GSE55374 and GSE59515) (34). The inability of AI therapy to inhibit the expression of the ER dysregulated gene set was significantly associated with poor response to therapy. Breast cancer patients whose tumours displayed a combined loss of the ER target gene signature following 3 months neoadjuvant treatment had a longer disease free- and overall- survival in comparison to patients whose tumours failed to regulate the expression levels of the gene signature in response to AI treatment (n=72, p=0.00339 and p=0.00155 respectively) (Fig. 5E). The target gene signature associated more strongly with survival than ER gene expression alone, although both together had improved predictive value (n=72, disease-free survival p=0.00076, overall survival p=0.00025) (Supplementary Fig. S11).

ER activity is not required to maintain growth of endocrine resistant distant metastatic tumours. In endocrine resistance, ligand independent ER activity is induced. This is exemplified by enhanced pSer118 ER and EGR3 observed in endocrine resistant cell lines (LetR and AnaR) (31)and in endocrine resistant local disease recurrence patient tissue (Fig. 6A; Supplementary Table S3). With the development of metastatic disease however there is a growing body of clinical evidence to suggest that a significant minority of tumours lose ER activity in comparison to the primary breast cancer (Fig. 6B). In this study, in matched primary and metastatic tumours from patients who have developed a recurrence on adjuvant treatment, almost half of the patients displayed loss of ER and/or PR expression in the metastatic tissue (n=10) (Fig 6C). Of note, loss of AR (androgen receptor) expression was also detected in some but not all patients following endocrine treatment (Supplementary Fig. S4). Consistent with the observation of loss of steroid receptors, loss of EGR3 protein expression was also found in metastatic tumours relative to the matched primary tissue following endocrine treatment (n=10, p=0.002 Supplementary Table S3) (Fig 6D). Furthermore, global analysis of transcript changes (RNAseq) between primary and metastatic ER positive AI treated patients revealed a loss of the ER target gene signature in both brain and liver metastatic tissue (Fig. 6E). Taken together these data provide evidence that a functional ER may not be required in selected patients for maintenance of metastatic tumours secondary to endocrine treatment.

DISCUSSION

Adaptation of ER-positive breast cancer tumours to a depleted estrogen environment has been studied extensively. Work presented here and studies from other groups have demonstrated continued ER functioning in the presence of AI treatment. Altered phosphorylation status, DNA mutations and functional alterations in the ER, including ligand-independent activation of the receptor have been observed (18-20). However, global analyses of ER-DNA binding events in AI resistant breast cancer have not been reported to date. Here we undertook ER ChIP-seq analysis in breast cancer cells

resistant to the AI letrozole. Loss of ER binding was observed in the AI resistant setting in comparison to that reported for the parental sensitive cells (27). Of interest, similar reductions in ER binding events have been reported previously for breast cancer cells resistant to tamoxifen (27). Data from this study and previous work from our group and others suggest that low levels of global ER binding observed in the AI resistant cells are unlikely to be due to either loss of ER phosphorylation at serine 118 (31) or reduced ER interactions with the pioneer factor FOXA1 (27). Furthermore, we observed no enhancement of ER binding with steroid treatment. Rather, adaptation to sustained estrogen deprivation resulted in a subset of classic ligand-dependent ER target genes becoming estrogen independent. The ER dysregulated gene signature included classic ER targets, GREB1 and TFF1, as well as genes with roles in growth response (EGR3) and differentiation (MREG).

ER may regulate specific gene sets in a promoter specific manner. Here analysis of transcription factor binding motifs revealed EREs to be enriched in the steroid independent setting, giving rise to ER dysregulated genes, whereas ER utilised alternative motifs, including forkhead and zinc finger binding motifs, for steroid dependent regulation. We have previously reported promoter specific binding for ER and its coactivator AIB1. Meta-analysis of several gene sets (39-41) demonstrated that ER/AIB1 regulated genes which contain either full or partial EREs contribute to pathways promoting tumour progression, relative to genes that do not contain an ER response element (29). Ligand independent ER signalling may therefore preferentially utilise EREs over other ER binding motifs to promote survival genes in the absence of steroid.

Associations between expression of the ER coactivator AIB1 and reduced disease free survival in AI treated patients has previously been reported (31). In this study, analysis of the globally identified ER and AIB1 interactome revealed steroid independent ER genes to be enriched for AIB1 in comparison to steroid regulated ER targets. *In vitro* molecular studies in models of AI resistance confirmed a role for AIB1 in ligand independent regulation of ER targets EGR3 and MREG and *ex vivo* clinical studies demonstrated a strong association between AIB1, EGR3 and ER in breast cancer

patients. These data implicate AIB1 in selective ligand independent ER transcriptional regulation.

This study focussed on the adaptive role of ER in response to AI therapy, but it should be noted that several other receptors are likely to contribute to the adaptive response. The androgen receptor for example is expressed both pre and post neoadjuvant AI therapy and may respond to the increased androgenic environment (42-44). Furthermore, growth factor receptor cross-talk has also been well documented in endocrine resistant breast cancer.

Loss of classic ER target gene expression following neoadjuvant AI treatment has been well described (38, 42, 43). We observed loss of the dysregulated ER gene signature at both 2 weeks and 3 months following neoadjuvant AI treatment in the majority of breast cancer patients examined, whereas a minority did not regulate gene expression in response to estrogen ablation. The inability of AI therapy to regulate tumour levels of the dysregulated ER gene set significantly associated with subsequent response to adjuvant treatment in ER positive breast cancer patients. These observations are consistent with recent reports of a dynamic four gene signature following short-term AI-treatment (2 weeks) as a predictive model for extended AI therapy (34). These observations support the concept that early dynamic ER gene expression alterations in response to treatment are important in determining long term responses to endocrine therapy. Indeed the clinical relevance, if any, of ligand independent ER activity following neoadjuvant AI will become evident as data from current trials, combining AI therapy with ER inhibitors (fulvestrant) for the neoadjuvant treatment of invasive breast cancer become available (clinicaltrials.gov NCT00921115 and NCT01953588).

Enhanced ligand independent ER activity, as manifest by pSer118 and EGR3 expression, was found in endocrine resistant local disease recurrent patient tumours in comparison to matched primary patient tissue. These observations are consistent with those previously reported in our cell line models of AI resistance (31). On development of metastatic cancer in patients who failed on adjuvant endocrine treatment, further

adaptations in ER signalling can be observed. Consistent with clinical studies from our group and others (21-23), we observed a loss of ER activity in a significant minority of metastatic tumours in comparison to matched primary tissue. Work from Hoefnagel *et al.* investigating receptor conversion at distant metastatic sites found that, conversion of the ER target PR was more frequent than alterations in ER expression itself and that overall steroid receptor conversion was more common in the liver and brain, in comparison to other metastatic sites (44, 45). In this study, reductions in protein expression of the ER target EGR3 were found at all metastatic sites examined. Furthermore, loss of the ER gene signature at transcript level was observed in metastatic liver and brain relative to the primary tumour. These data are consistent with the concept that selected metastatic tumours can adapt to become fully independent of ER activity.

In summary work from this study suggests that estrogen ablation leads to an adaptive ER response. An initial enhanced ligand independent activity seen following neoadjuvant treatment and local endocrine resistant disease can give way to loss of ER signalling in the distant metastatic setting. ER adaptability to endocrine therapy has several clinical consequences; firstly, the need for more efficient drugs to completely block ER signalling during first-line treatment; and secondly, the need to re-assess where possible, the ER status during disease progression, particularly at the metastatic stage, in order to select the most appropriate treatment.

Authors' Contribution

Conception and design: D.V., J.M., L.Y.

Development of methodology: D.V., J.M., L.Y.

Acquisition of data: D.V., J.M., A.M.R., L.H., S.P., A.T.

Analysis and interpretation of data (e.g., statistical analysis, biostatistics, computational analysis): D.V., J.M., A.F., Y.H., A.S., L.Y.

Writing, review, and/or revision of the manuscript: D.V., J.M., J.M.D., L.Y.

Study supervision: A.H., L.Y.

Acknowledgements

The authors thank Prof. William Miller for his technical expertise and review of the manuscript. We kindly acknowledge the funding support from Science Foundation Ireland (08-IN1-B1853), the Health Research Board of Ireland (HRB/POR/2012/101) and Breast Cancer Campaign (2013MaySP022). This material is also based upon works supported by the Irish Cancer Society Collaborative Cancer Research Centre grant, CCRC13GAL. A.H.S., A.T. and J.M.D. are grateful for funding from Breakthrough Breast Cancer.

REFERENCES

1. Miller WR, Larionov AA. Understanding the mechanisms of aromatase inhibitor resistance. Breast Cancer Res. 2012;14:201.
2. Fox EM, Arteaga CL, Miller TW. Abrogating endocrine resistance by targeting ERalpha and PI3K in breast cancer. Front Oncol. 2012;2:145.
3. Johnston SR, Dowsett M. Aromatase inhibitors for breast cancer: lessons from the laboratory. Nat Rev Cancer. 2003;3:821-31.
4. Fleeman N, Bagust A, Boland A, Dickson R, Dundar Y, Moonan M, et al. Lapatinib and trastuzumab in combination with an aromatase inhibitor for the first-line treatment of metastatic hormone receptor-positive breast cancer which over-expresses human epidermal growth factor 2 (HER2): a systematic review and economic analysis. Health Technol Assess. 2011;15:1-93, iii-iv.
5. Chumsri S, Sabnis GJ, Howes T, Brodie AM. Aromatase inhibitors and xenograft studies. Steroids. 2011;76:730-5.
6. De Laurentiis M, Arpino G, Massarelli E, Ruggiero A, Carlomagno C, Ciardiello F, et al. A meta-analysis on the interaction between HER-2 expression and response to endocrine treatment in advanced breast cancer. Clin Cancer Res. 2005;11:4741-8.
7. Ma CX, Crowder RJ, Ellis MJ. Importance of PI3-kinase pathway in response/resistance to aromatase inhibitors. Steroids. 2011;76:750-2.
8. Creighton CJ, Fu X, Hennessy BT, Casa AJ, Zhang Y, Gonzalez-Angulo AM, et al. Proteomic and transcriptomic profiling reveals a link between the PI3K pathway and lower estrogen-receptor (ER) levels and activity in ER+ breast cancer. Breast Cancer Res. 2010;12:R40.
9. Miller TW, Hennessy BT, Gonzalez-Angulo AM, Fox EM, Mills GB, Chen H, et al. Hyperactivation of phosphatidylinositol-3 kinase promotes escape from hormone dependence in estrogen receptor-positive human breast cancer. J Clin Invest. 2010;120:2406-13.
10. Bhat-Nakshatri P, Campbell RA, Patel NM, Newton TR, King AJ, Marshall MS, et al. Tumour necrosis factor and PI3-kinase control oestrogen receptor alpha protein level and its transrepression function. Br J Cancer. 2004;90:853-9.
11. Campbell RA, Bhat-Nakshatri P, Patel NM, Constantinidou D, Ali S, Nakshatri H. Phosphatidylinositol 3-kinase/AKT-mediated activation of estrogen receptor alpha: a new model for anti-estrogen resistance. J Biol Chem. 2001;276:9817-24.
12. Miller TW, Balko JM, Fox EM, Ghazoui Z, Dunbier A, Anderson H, et al. ERalpha-dependent E2F transcription can mediate resistance to estrogen deprivation in human breast cancer. Cancer Discov. 2011;1:338-51.
13. Ingle JN, Suman VJ, Rowland KM, Mirchandani D, Bernath AM, Camoriano JK, et al. Fulvestrant in women with advanced breast cancer after progression on prior aromatase inhibitor therapy: North Central Cancer Treatment Group Trial N0032. J Clin Oncol. 2006;24:1052-6.
14. Perey L, Paridaens R, Hawle H, Zaman K, Nole F, Wildiers H, et al. Clinical benefit of fulvestrant in postmenopausal women with advanced breast cancer and primary or acquired resistance to aromatase inhibitors: final results of phase II Swiss Group for Clinical Cancer Research Trial (SAKK 21/00). Ann Oncol. 2007;18:64-9.

15. Weis KE, Ekena K, Thomas JA, Lazennec G, Katzenellenbogen BS. Constitutively active human estrogen receptors containing amino acid substitutions for tyrosine 537 in the receptor protein. Mol Endocrinol. 1996;10:1388-98.
16. White R, Sjoberg M, Kalkhoven E, Parker MG. Ligand-independent activation of the oestrogen receptor by mutation of a conserved tyrosine. EMBO J. 1997;16:1427-35.
17. Roodi N, Bailey LR, Kao WY, Verrier CS, Yee CJ, Dupont WD, et al. Estrogen receptor gene analysis in estrogen receptor-positive and receptor-negative primary breast cancer. J Natl Cancer Inst. 1995;87:446-51.
18. Robinson DR, Wu YM, Vats P, Su F, Lonigro RJ, Cao X, et al. Activating ESR1 mutations in hormone-resistant metastatic breast cancer. Nat Genet. 2013;45:1446-51.
19. Jeselsohn R, Yelensky R, Buchwalter G, Frampton GM, Meric-Bernstam F, Gonzalez-Angulo AM, et al. Emergence of constitutively active estrogen receptor-alpha mutations in pretreated advanced estrogen receptor positive breast cancer. Clin Cancer Res. 2014.
20. Ross-Innes CS, Stark R, Teschendorff AE, Holmes KA, Ali HR, Dunning MJ, et al. Differential oestrogen receptor binding is associated with clinical outcome in breast cancer. Nature. 2012;481:389-93.
21. McBryan J, Theissen SM, Byrne C, Hughes E, Cocchiglia S, Sande S, et al. Metastatic progression with resistance to aromatase inhibitors is driven by the steroid receptor coactivator SRC-1. Cancer Res. 2012;72:548-59.
22. Broom RJ, Tang PA, Simmons C, Bordeleau L, Mulligan AM, O'Malley FP, et al. Changes in estrogen receptor, progesterone receptor and Her-2/neu status with time: discordance rates between primary and metastatic breast cancer. Anticancer Res. 2009;29:1557-62.
23. Arnedos M, Drury S, Afentakis M, A'Hern R, Hills M, Salter J, et al. Biomarker changes associated with the development of resistance to aromatase inhibitors (AIs) in estrogen receptor-positive breast cancer. Ann Oncol. 2014.
24. Bronzert DA, Greene GL, Lippman ME. Selection and characterization of a breast cancer cell line resistant to the antiestrogen LY 117018. Endocrinology. 1985;117:1409-17.
25. Redmond AM, Bane FT, Stafford AT, McIlroy M, Dillon MF, Crotty TB, et al. Coassociation of estrogen receptor and p160 proteins predicts resistance to endocrine treatment; SRC-1 is an independent predictor of breast cancer recurrence. Clin Cancer Res. 2009;15:2098-106.
26. Schmidt D, Wilson MD, Spyrou C, Brown GD, Hadfield J, Odom DT. ChIP-seq: using high-throughput sequencing to discover protein-DNA interactions. Methods. 2009;48:240-8.
27. Hurtado A, Holmes KA, Ross-Innes CS, Schmidt D, Carroll JS. FOXA1 is a key determinant of estrogen receptor function and endocrine response. Nat Genet. 2011;43:27-33.
28. Redmond AM, Byrne C, Bane FT, Brown GD, Tibbitts P, O'Brien K, et al. Genomic interaction between ER and HMGB2 identifies DDX18 as a novel driver of endocrine resistance in breast cancer cells. Oncogene. 2014.
29. Langmead B, Trapnell C, Pop M, Salzberg SL. Ultrafast and memory-efficient alignment of short DNA sequences to the human genome. Genome Biol. 2009;10:R25.

30. Zhang Y, Liu T, Meyer CA, Eeckhoute J, Johnson DS, Bernstein BE, et al. Model-based analysis of ChIP-Seq (MACS). Genome Biol. 2008;9:R137.
31. O'Hara J, Vareslija D, McBryan J, Bane F, Tibbitts P, Byrne C, et al. AIB1:ERalpha Transcriptional Activity Is Selectively Enhanced in Aromatase Inhibitor-Resistant Breast Cancer Cells. Clin Cancer Res. 2012;18:3305-15.
32. Dillon MF, Stafford AT, Kelly G, Redmond AM, McIlroy M, Crotty TB, et al. Cyclooxygenase-2 predicts adverse effects of tamoxifen: a possible mechanism of role for nuclear HER2 in breast cancer patients. Endocr Relat Cancer. 2008;15:745-53.
33. Myers E, Hill AD, Kelly G, McDermott EW, O'Higgins NJ, Buggy Y, et al. Associations and interactions between Ets-1 and Ets-2 and coregulatory proteins, SRC-1, AIB1, and NCoR in breast cancer. Clin Cancer Res. 2005;11:2111-22.
34. Turnbull AK, Arthur LM, Renshaw L, Larionov AA, Kay C, Dunbier AK, et al. Accurate Prediction and Validation of Response to Endocrine Therapy in Breast Cancer. J Clin Oncol. 2015.
35. Turnbull AK, Kitchen RR, Larionov AA, Renshaw L, Dixon JM, Sims AH. Direct integration of intensity-level data from Affymetrix and Illumina microarrays improves statistical power for robust reanalysis. BMC Med Genomics. 2012;5:35.
36. Masri S, Phung S, Wang X, Wu X, Yuan YC, Wagman L, et al. Genome-wide analysis of aromatase inhibitor-resistant, tamoxifen-resistant, and long-term estrogen-deprived cells reveals a role for estrogen receptor. Cancer Res. 2008;68:4910-8.
37. Zwart W, Theodorou V, Kok M, Canisius S, Linn S, Carroll JS. Oestrogen receptor-co-factor-chromatin specificity in the transcriptional regulation of breast cancer. EMBO J. 2011;30:4764-76.
38. Miller WR, Larionov A, Anderson TJ, Evans DB, Dixon JM. Sequential changes in gene expression profiles in breast cancers during treatment with the aromatase inhibitor, letrozole. Pharmacogenomics J. 2010;12:10-21.
39. Lanz RB, Bulynko Y, Malovannaya A, Labhart P, Wang L, Li W, et al. Global characterization of transcriptional impact of the SRC-3 coregulator. Mol Endocrinol. 2010;24:859-72.
40. Ross-Innes CS, Stark R, Holmes KA, Schmidt D, Spyrou C, Russell R, et al. Cooperative interaction between retinoic acid receptor-alpha and estrogen receptor in breast cancer. Genes Dev. 2010;24:171-82.
41. Welboren WJ, van Driel MA, Janssen-Megens EM, van Heeringen SJ, Sweep FC, Span PN. ChIP-Seq of ER-alpha and RNA polymerase II defines genes differentially responding to ligands. The EMBO Journal. 2009;28:1418-28.
42. Mackay A, Urruticoechea A, Dixon JM, Dexter T, Fenwick K, Ashworth A, et al. Molecular response to aromatase inhibitor treatment in primary breast cancer. Breast Cancer Res. 2007;9:R37.
43. Mello-Grand M, Singh V, Ghimenti C, Scatolini M, Regolo L, Grosso E, et al. Gene expression profiling and prediction of response to hormonal neoadjuvant treatment with anastrozole in surgically resectable breast cancer. Breast Cancer Res Treat. 2010;121:399-411.
44. Hoefnagel LD, Moelans CB, Meijer SL, van Slooten HJ, Wesseling P, Wesseling J, et al. Prognostic value of estrogen receptor alpha and progesterone receptor conversion in distant breast cancer metastases. Cancer. 2012;118:4929-35.

45. Hoefnagel LD, van de Vijver MJ, van Slooten HJ, Wesseling P, Wesseling J, Westenend PJ, et al. Receptor conversion in distant breast cancer metastases. Breast Cancer Res. 2010;12:R75.
46. Kong SL, Li G, Loh SL, Sung WK, Liu ET. Cellular reprogramming by the conjoint action of ERalpha, FOXA1, and GATA3 to a ligand-inducible growth state. Mol Syst Biol. 2011;7:526.

LEGENDS

FIGURE LEGENDS

Figure 1. The estrogen receptor remains active in breast cancer following AI therapy. **A,** Graphic illustrates tumour sampling before and after neoadjuvant AI therapy. Representative images show pSer118 ER immunohistochemistry in matched pre- and post- AI treatment tumour samples. The staining was scored (Allred method) and graphed for matched tumour samples from eight patients. pSer118 expression significantly increased during AI treatment (n=8, paired t-test, p=0.002). **B,** Growth assays under steroid-depleted conditions were performed in AI-sensitive (MCF7, MCF7-Aro) and AI-resistant (LetR and AnaR) cells. Transient transfection with non-targeting (NT) or ER-specific (ER KD) siRNA was used to achieve ER knockdown, as confirmed by western blot. Graphs show mean cell number ± SEM (n=3) and demonstrate the significant contribution of ligand-independent ER activity to growth of AI-resistant cells. **p<0.01, *p<0.05, n.s. not significant.

Figure 2. Identifying the ER transcriptome in AI-resistant breast cancer cells. **A,** ER ChIP-seq analysis in LetR cells revealed comparable binding in vehicle treated and androstenedione treated samples as illustrated by the ER binding heat map (±2.5kb of peak centre) and the Venn diagram depicting the number of ER binding peaks. **B,** Pie charts show enrichment of EREs within ER binding peaks which were not dependent on steroid treatment. **C,** Table shows over-represented transcription factor binding motifs within ER peaks. EREs are enriched in steroid-independent peaks whereas FOXA1 motifs are enriched in steroid-dependent peaks. **D,** Steroid-independent ER target genes identified from ER ChIP-seq in LetR cells were filtered by comparison to two expression data sets (36, 46) as summarised by the flowchart. Filtering was based on genes displaying increased expression in response to steroid in MCF7 cells and in MCF7-Aro cells and expression in LetR cells. This analysis led to the identification of 7 genes of interest which had become steroid dysregulated in AI resistant cells (TFF1, GREB1, EGR3, MREG, SIAH2, MYB, TPD52L1).

Figure 3. ER regulates EGR3 and MREG expression independently of steroids in LetR cells. **A,** Images from UCSC genome browser of LetR ER ChIP-seq vehicle sample depicting EGR3 and MREG ER binding peaks with EREs. **B,** q-PCR of ER ChIP in MCF7 (grey bars) and LetR (black bars) cells revealed recruitment of ER to EGR3 and MREG genes. IgG was used as an internal control. Treatments were vehicle (V), estrogen (E) and androstenedione (A). ER ChIP shows ER binding is steroid-independent in LetR cells compared to MCF7 cells. **C,** EGR3 and MREG expression is regulated by ER. LetR cells were transiently transfected with ER siRNA and mRNA was analysed by q-PCR. Protein expression was also verified by western blot. β-Actin is used as loading control. **D,** High expression of EGR3 and MREG becomes steroid independent in LetR cells. MCF7 and LetR cells were treated with either E or A, and mRNA and protein were analysed by q-PCR or western blot, respectively. Results are mean ± SEM, n=3. **p<0.01,*p<0.05, n.s. not significant.

Figure 4. AIB1 co-activates ER to regulate expression of EGR3 and MREG in AI resistance. **A,** ER binding peaks from LetR cells were compared to AIB1 binding peaks from MCF7 cells (45). Pie charts illustrate the overlap between ER and AIB1 peaks in treated and untreated LetR cells. **B,** q-PCR of AIB1 ChIP in MCF7 (grey) and LetR (black) cells revealed recruitment of AIB1 to EGR3 and MREG promoters. IgG was used as an internal control. Treatments were vehicle (V), estrogen (E) and androstenedione (A). AIB1 ChIP shows AIB1 binding is steroid-independent in LetR cells compared to MCF7 cells. **C,** EGR3 and MREG expression is regulated by AIB1. LetR cells were transiently transfected with AIB1 siRNA and mRNA was analysed by q-PCR. Protein expression was verified by western blot. β-Actin is used as loading control. Results are mean ± SEM, n=3. *p<0.05, n.s. not significant. **D,** Patient tissue microarray (TMA) was stained for ER, AIB1 and EGR3. Images show representative positive and negative staining. Significant associations were detected between all 3 proteins using Fisher's exact test.

Figure 5. Maintained expression of steroid-dysregulated genes following AI treatment associates with poor outcomes. **A,** Tumours were sampled before, during and after neoadjuvant AI therapy (34, 38) as illustrated. **B,** Box plots display expression changes of steroid dysregulated genes in neoadjuvant AI treated patients (n=50 patients). All genes display a decrease in expression with the exception of EGR3 which increases at 3 months. Paired t-tests pre-treated vs 3 months. **C,** Protein expression confirms a significant increase in EGR3 expression following 3 months AI treatment. Representative IHC images are shown. All images were Allred-scored and results are displayed on the graph (n=9 patients, paired t-test, p=0.0002). **D,** MCF7-Aro cells treated with androstenedione (A) and anastrozole (AI) were analysed by q-PCR for EGR3 expression. Consistent with patient data, EGR3 expression initially decreased and subsequently increased significantly in response to AI treatment, n=3, mean ± SEM, **p<0.01,*p<0.05). **E,** Ranked sum of steroid dysregulated gene expression changes are associated with poor prognosis. Red=increased and green=decreased at 3 months relative to pre-treatment for 72 AI-treated patients (34). White-grey-black bars indicate significance of all possible cut points from p=1 to 0.001. Kaplan Meier according to expression of the ER gene signature. Reductions in the ER gene signature following neoadjuvant AI therapy associate with increased disease free and overall survival in AI treated breast cancer patients (n=72, p= 0.00339 and p=0.00155, respectively).

Figure 6. Early adaptive changes are lost in distant metastatic tumours indicating a switch away from ER signalling. **A,** pSer118 ER and EGR3 protein expression is increased in local recurrent tumours relative to their matched primary tumours (n=6 individual patients). Patient details are provided in Supplementary Table S3. **B,** Graphic illustrating the dynamic changes in ER activity observed during breast cancer disease progression in select patients. **C,** ER and PR status is graphed for matched primary and metastatic endocrine treated tumours (n= 10 breast cancer patients). Solid lines: AI treated patients; dashed lines: tamoxifen treated patients. **D,** EGR3 protein expression is reduced in metastatic tumours of patients that recurred while on endocrine treatment

(n=9, p=0.002). Solid lines: AI treated patients; dashed lines: tamoxifen treated patients. Representative images of the EGR3 staining of matched patient samples are shown. **E,** RNA-seq data obtained from ER positive matched primary and metastatic breast cancer patient tumours following AI treatment (n=3). Heat map illustrates ER gene signature expression as determined by RNAseq in primary and metastatic breast cancer tumours (n=3).

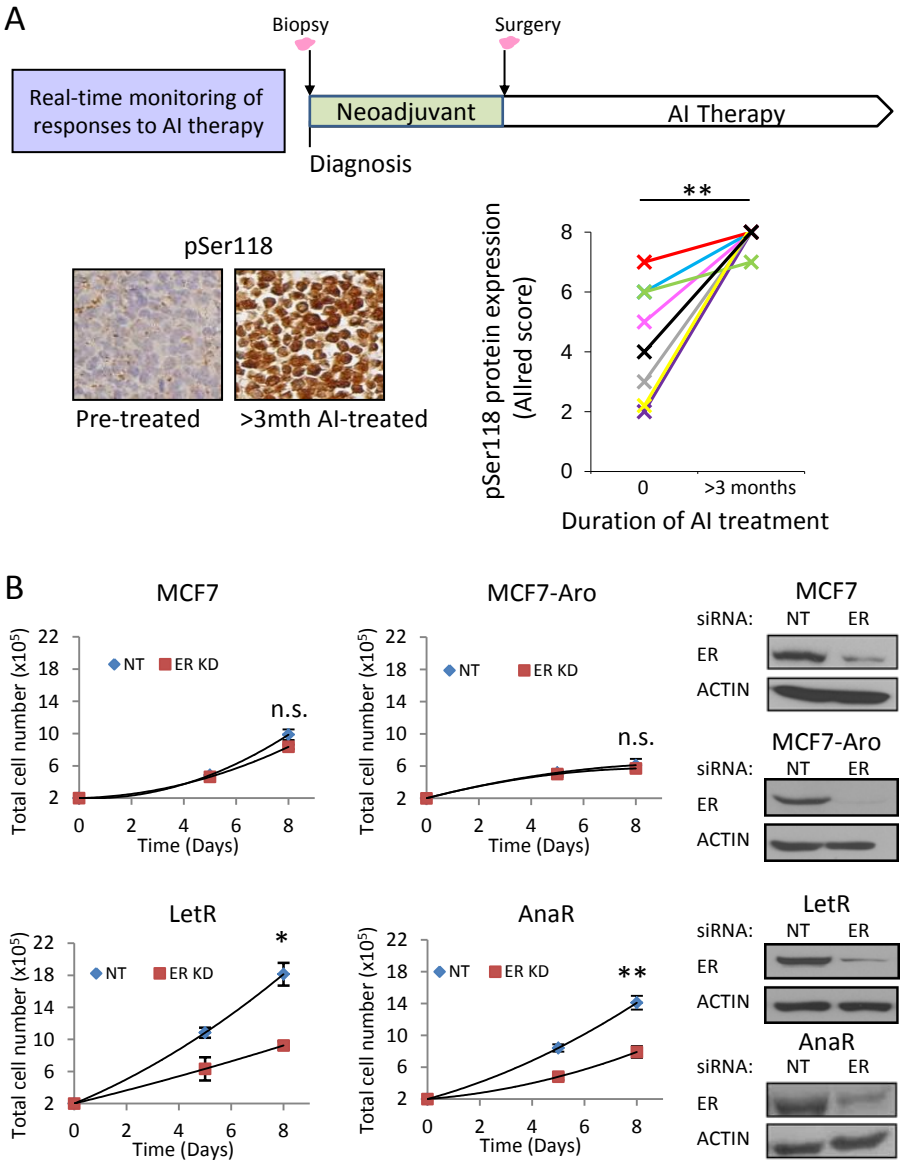
A
Biopsy
Surgery
Real-time monitoring of responses to AI therapy
Neoadjuvant
AI Therapy
Diagnosis
pSer118
Pre-treated
>3mth AI-treated
**
pSer118 protein expression (Allred score)
0
>3 months
Duration of AI treatment
B
MCF7
MCF7-Aro
LetR
AnaR
NT
ER KD
n.s.
*
**
Total cell number (x10⁵)
Time (Days)
siRNA:
ER
ACTIN

Figure 1

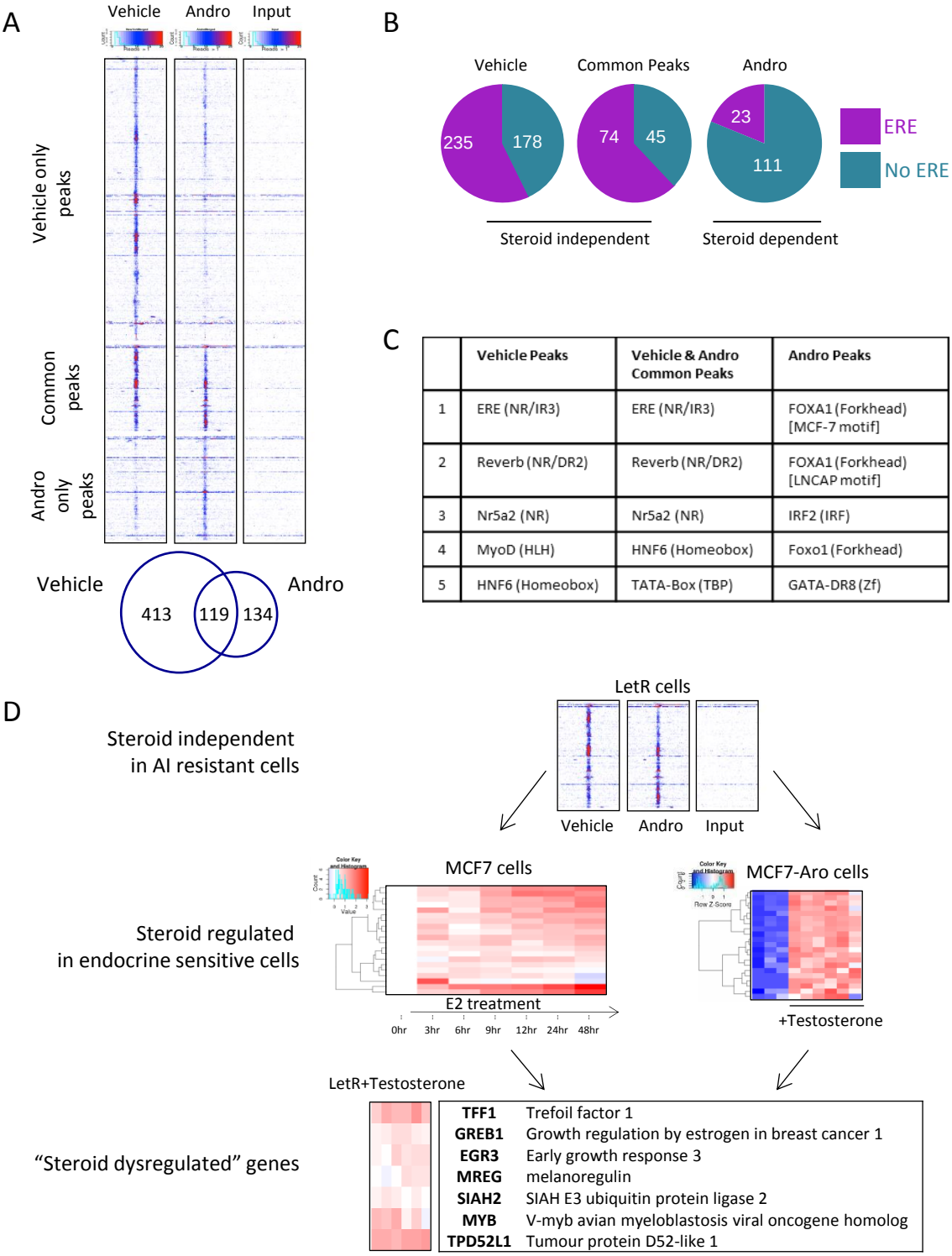

	Vehicle Peaks	Vehicle & Andro Common Peaks	Andro Peaks
1	ERE (NR/IR3)	ERE (NR/IR3)	FOXA1 (Forkhead) [MCF-7 motif]
2	Reverb (NR/DR2)	Reverb (NR/DR2)	FOXA1 (Forkhead) [LNCAP motif]
3	Nr5a2 (NR)	Nr5a2 (NR)	IRF2 (IRF)
4	MyoD (HLH)	HNF6 (Homeobox)	Foxo1 (Forkhead)
5	HNF6 (Homeobox)	TATA-Box (TBP)	GATA-DR8 (Zf)

TFF1	Trefoil factor 1
GREB1	Growth regulation by estrogen in breast cancer 1
EGR3	Early growth response 3
MREG	melanoregulin
SIAH2	SIAH E3 ubiquitin protein ligase 2
MYB	V-myb avian myeloblastosis viral oncogene homolog
TPD52L1	Tumour protein D52-like 1

Figure 2

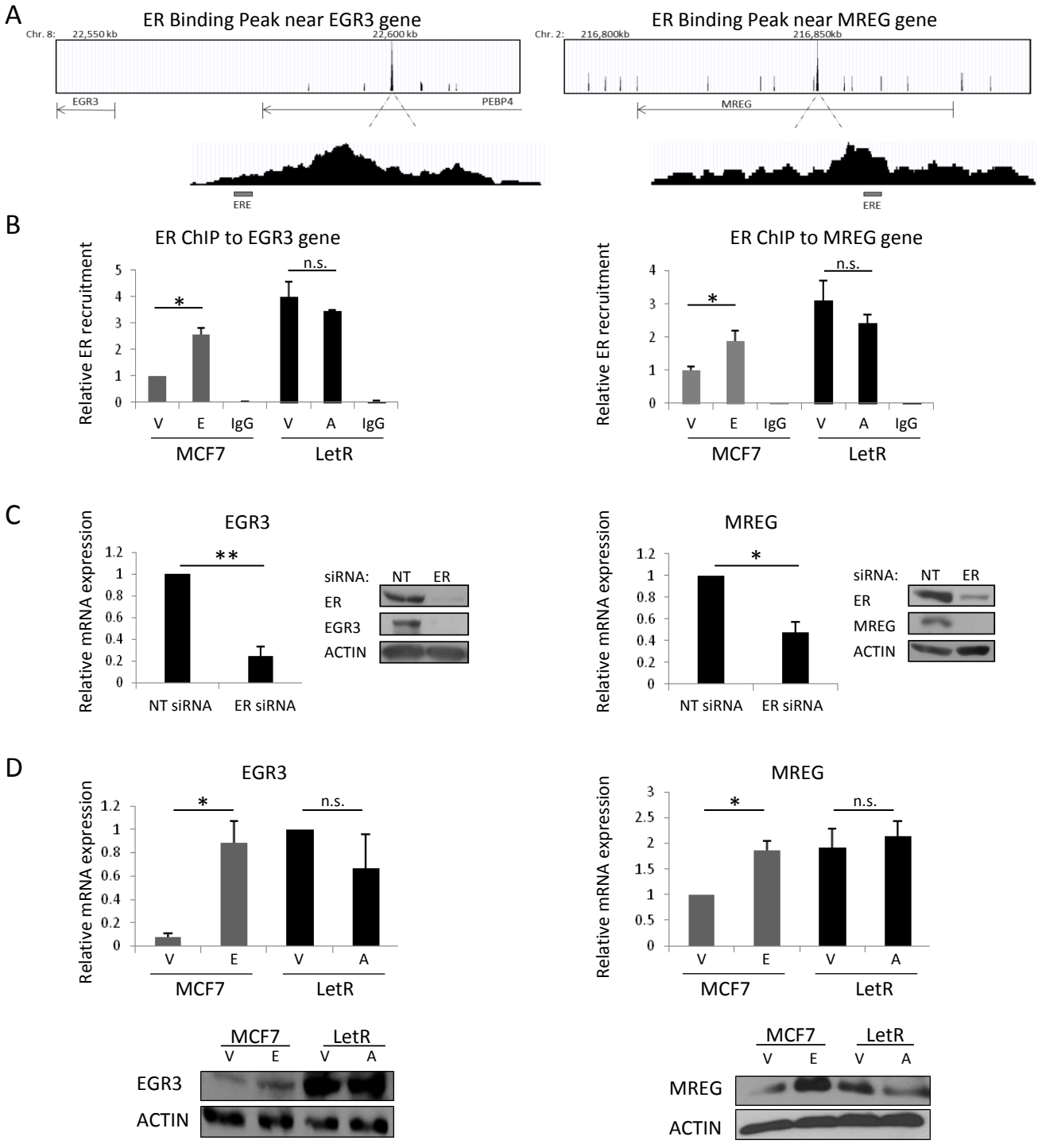
A
ER Binding Peak near EGR3 gene
Chr. 8: 22,550 kb
22,600 kb
EGR3
PEBP4
ERE
ER Binding Peak near MREG gene
Chr. 2: 216,800kb
216,850kb
MREG
ERE
B
ER ChIP to EGR3 gene
Relative ER recruitment
n.s.
*
V E IgG V A IgG
MCF7
LetR
ER ChIP to MREG gene
Relative ER recruitment
n.s.
*
V E IgG V A IgG
MCF7
LetR
C
EGR3
Relative mRNA expression
**
NT siRNA
ER siRNA
siRNA: NT ER
ER
EGR3
ACTIN
MREG
Relative mRNA expression
*
NT siRNA
ER siRNA
siRNA: NT ER
ER
MREG
ACTIN
D
EGR3
Relative mRNA expression
*
n.s.
V E V A
MCF7
LetR
MCF7 LetR
V E V A
EGR3
ACTIN
MREG
Relative mRNA expression
*
n.s.
V E V A
MCF7
LetR
MCF7 LetR
V E V A
MREG
ACTIN

Figure 3

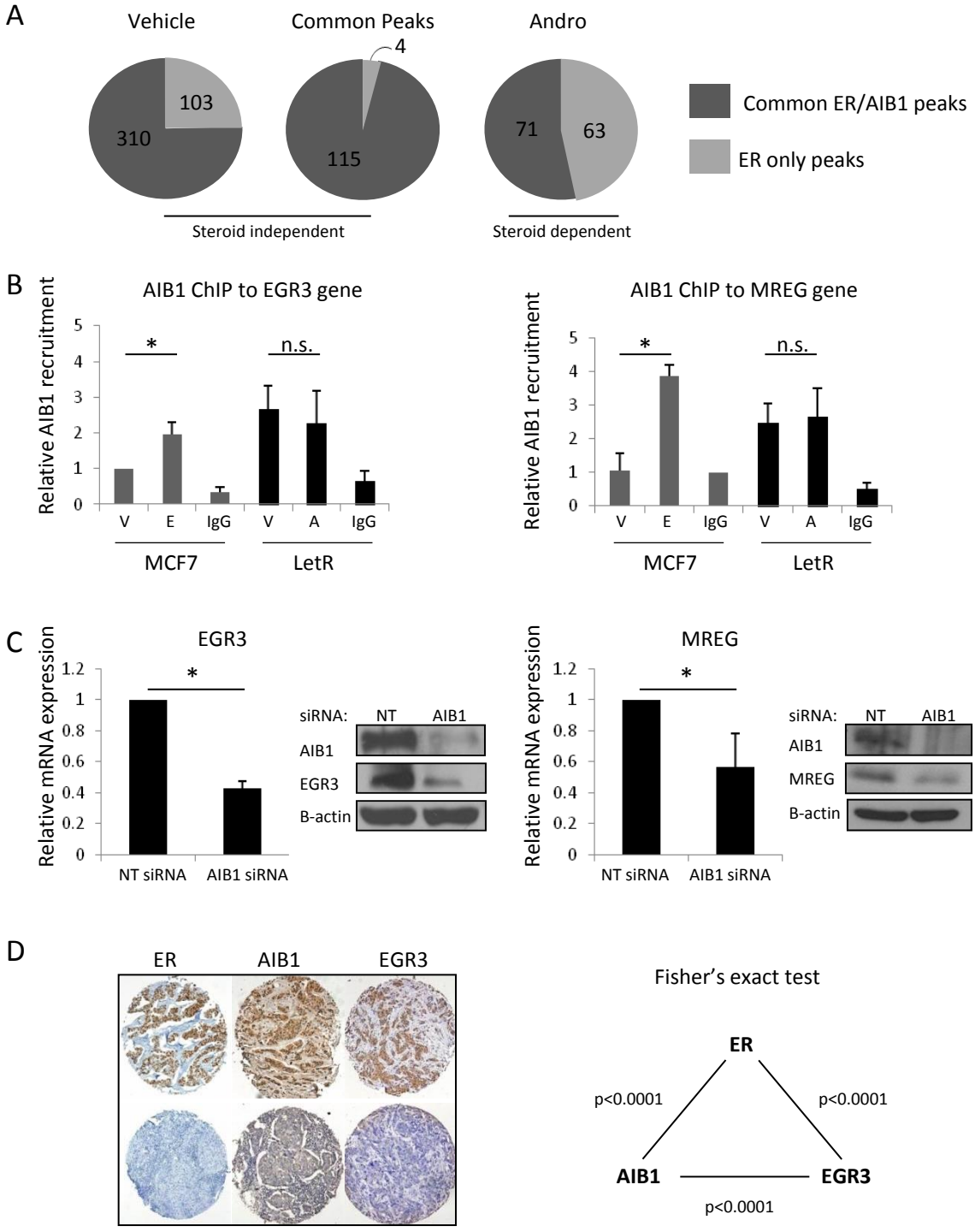
A
Vehicle
Common Peaks
Andro
103
310
4
115
71
63
Common ER/AIB1 peaks
ER only peaks
Steroid independent
Steroid dependent
B
AIB1 ChIP to EGR3 gene
AIB1 ChIP to MREG gene
Relative AIB1 recruitment
*
n.s.
V
E
IgG
A
MCF7
LetR
C
EGR3
MREG
Relative mRNA expression
NT siRNA
AIB1 siRNA
siRNA:
NT
AIB1
EGR3
MREG
B-actin
D
ER
AIB1
EGR3
Fisher's exact test
p<0.0001
p<0.0001
p<0.0001

Figure 4

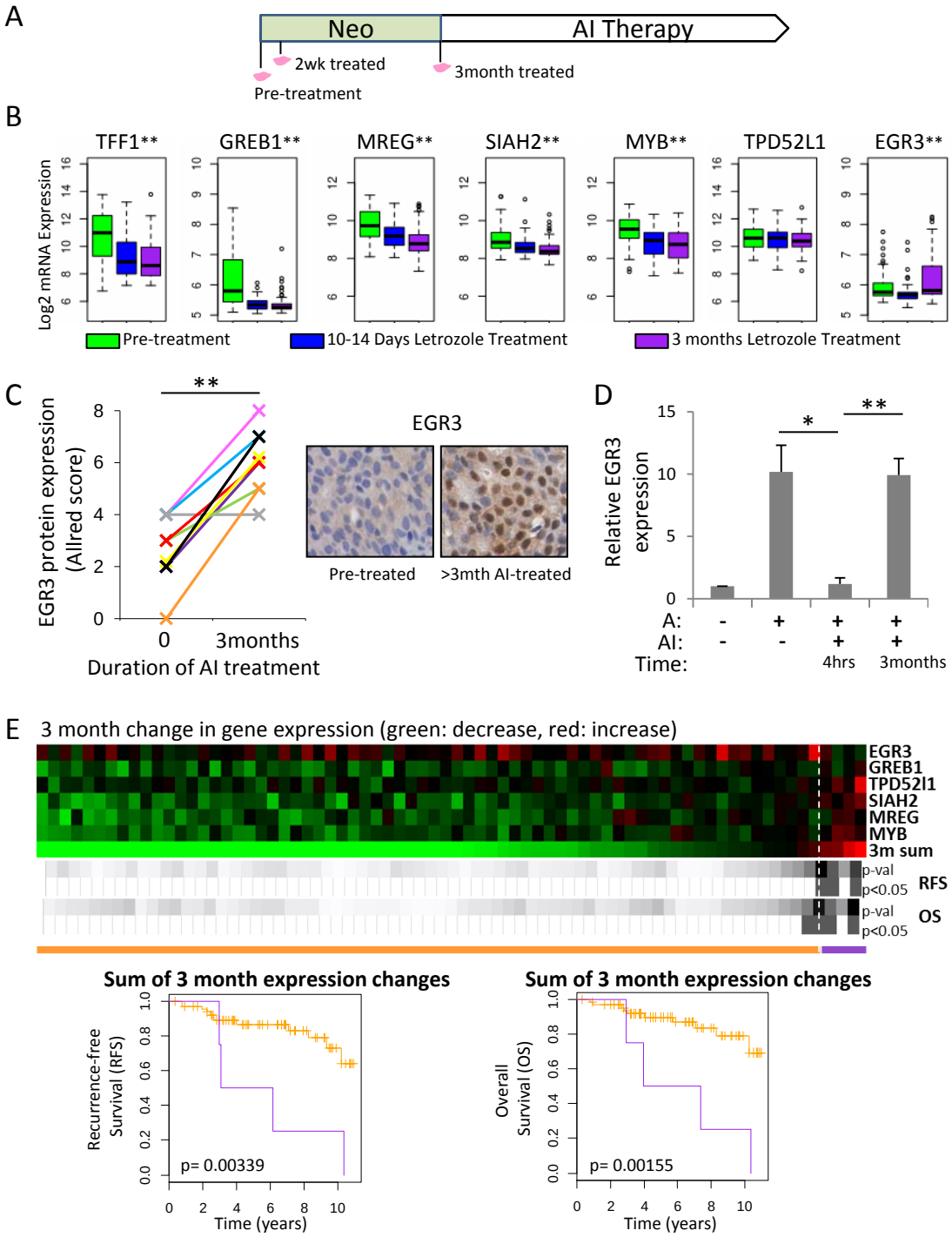
A
Neo
AI Therapy
2wk treated
3month treated
Pre-treatment
B
TFF1**
GREB1**
MREG**
SIAH2**
MYB**
TPD52L1
EGR3**
Log2 mRNA Expression
Pre-treatment
10-14 Days Letrozole Treatment
3 months Letrozole Treatment
C
**
EGR3 protein expression (Allred score)
0
3months
Duration of AI treatment
EGR3
Pre-treated
>3mth AI-treated
D
*
**
Relative EGR3 expression
A:
AI:
Time:
4hrs
3months
E
3 month change in gene expression (green: decrease, red: increase)
EGR3
GREB1
TPD52l1
SIAH2
MREG
MYB
3m sum
p-val
p<0.05
RFS
OS
Sum of 3 month expression changes
Recurrence-free Survival (RFS)
p= 0.00339
Time (years)
Sum of 3 month expression changes
Overall Survival (OS)
p= 0.00155
Time (years)

Figure 5

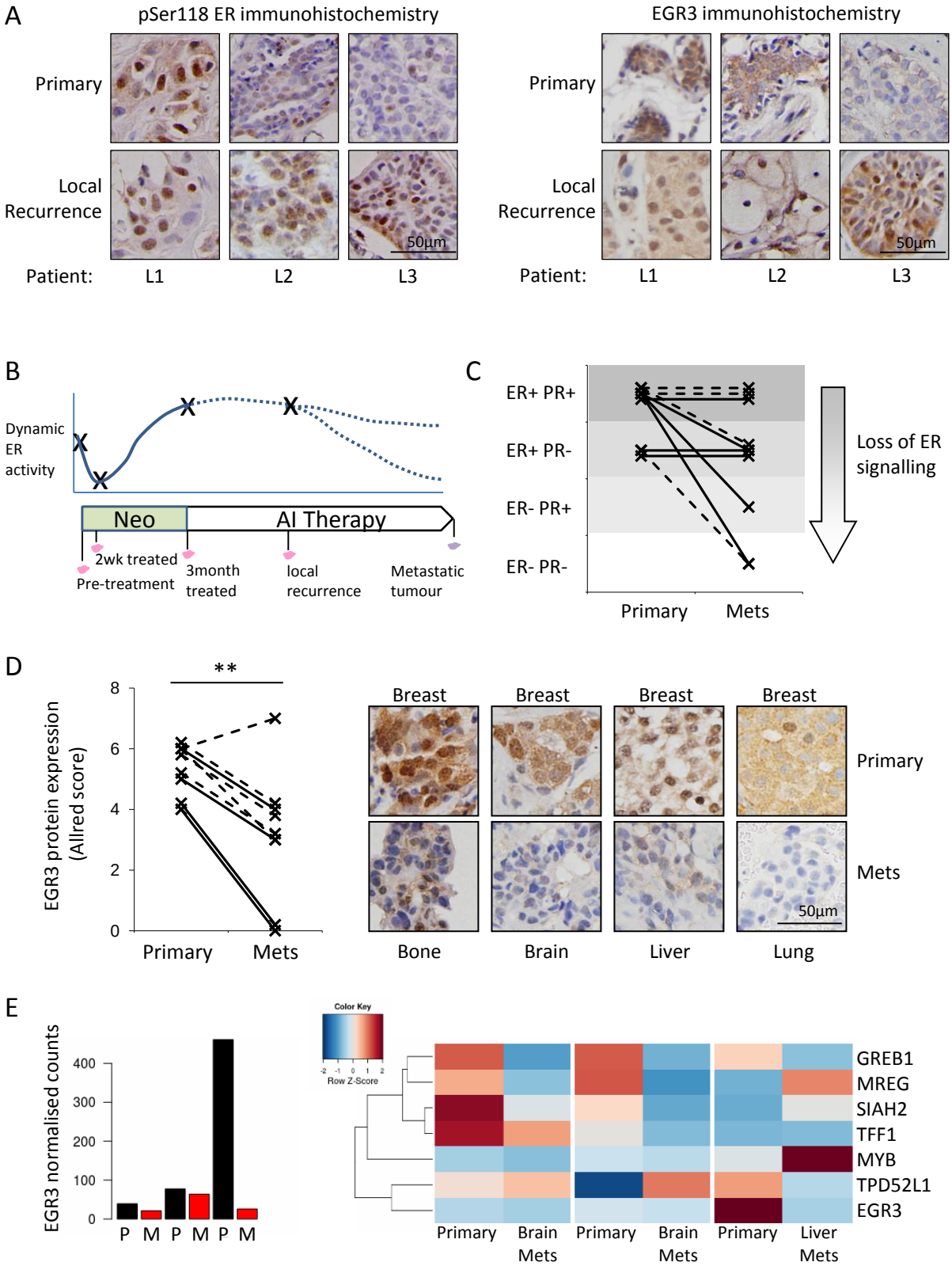
A
pSer118 ER immunohistochemistry
EGR3 immunohistochemistry
Primary
Local Recurrence
Patient:
L1
L2
L3
50µm
B
Dynamic ER activity
Neo
AI Therapy
2wk treated
Pre-treatment
3month treated
local recurrence
Metastatic tumour
C
ER+ PR+
ER+ PR-
ER- PR+
ER- PR-
Loss of ER signalling
Primary
Mets
D
**
EGR3 protein expression (Allred score)
Primary
Mets
Breast
Bone
Brain
Liver
Lung
E
EGR3 normalised counts
P M P M P M
Color Key
Row Z-Score
GREB1
MREG
SIAH2
TFF1
MYB
TPD52L1
EGR3
Primary
Brain Mets
Liver Mets

Figure 6